Semiconductor Optoelectronics
ISSN: 1001-5868

ALL-OPTICAL BPSK LABEL RECOGNITION IN PHOTONIC SWITCHING NETWORKS USING CASCADED MMI STRUCTURES ON SILICON-ON-INSULATOR PLATFORM

Thi Hong Loan Nguyen[a], Duy Tien Le[b], Le Minh Duong[c] and Trung Thanh Le[b]*,

[a]Hanoi University of Natural Resources and Environment (HUNRE), Hanoi, 1000000, Vietnam

[b]International School (VNU-IS), Vietnam National University (VNU), Hanoi, 1000000, Vietnam. .

[c]VNU University of Engineering and Technology (VNU-UET), Vietnam National University (VNU), Hanoi, 1000000, Vietnam

Abstract:

This research introduces optical circuits based on multimode interference (MMI) structures for the recognition of Binary Phase Shift Keying (BPSK) coded labels. The proposed circuits employ 1x2, 4x4 and 2x2 cascaded MMIs. The performance of these devices is rigorously analyzed and validated using the finite-difference beam propagation (BPM) and Eigenmode Expansion (EME) method. The design is based on the silicon on insulator (SOI) platform, which is suitable for the existing CMOS technology. The new proposed design has advantages of low loss, compactness, high bandwidth and large fabrication tolerance compared to the recent research published in the literature based on X-junction couplers. The fabrication tolerance for the MMI length is ±100 nm and the bandwidth is about 15nm.

Keywords: BPSK modulation, Multimode interference (MMI), integrated optics, silicon photonics, and label recognition

1. Introduction

In the realm of high-speed broadband networks, there is a growing interest in the application of optical processing for switching and routing [1]. Beyond its potential for transparent switching irrespective of modulation format, optical processing is particularly appealing due to its low power dissipation, a characteristic that has garnered significant attention over the past decade. The exploration of flexible elastic networks and elastic data center interconnections has led to in-depth studies on high Quality of Service (QoS) control, including the establishment of an optical-as-a-service architecture.

Within the domain of photonic networks, optical label switching networks emerge as practical solutions. These networks leverage optical labels to simplify routing processing, offering the advantage of low power dissipation across the network [2]. Label switching nodes

within these networks necessitate various optical signal processing functionalities, including label extraction, recognition, and swapping. Numerous studies have explored methods for representing labels in both time and spectral domains, as well as label recognition employing optical technologies [3].

In label recognition systems, integrated-optic passive waveguide devices have proven instrumental in leveraging optical interference among guided waves. These devices have demonstrated the capability to handle multiple labels simultaneously [4]. The previous research has delved into the study of optical waveguide devices designed to recognize optical codes in binary-phase-shift-keying (BPSK) and QPSK (Quadrature Phase Shift Keying) forms [1, 5, 6]. The employed self-routing scheme incorporates a reference pulse using coded labels, and the device architecture comprises asymmetric X-junction couplers arranged in a tree structure. This configuration is advantageous as it enables the identification of an optical phase difference of π with a single asymmetric X-junction coupler [7]. However, the X-junction coupler requires an extremely high fabrication technology to achieve the desired coupling coefficients. In addition, the bandwidth of the coupler is low compared with the device based on the MMIs.

To achieve large-capacity and high-speed photonic networks, the preference is for rapid optical processing without the need for conversion to electric signals [8]. Photonic routing has garnered significant attention as a solution to overcome the bottleneck in routing functions within high-speed networks. Specifically, there is considerable interest in photonic label routing networks, which are anticipated to facilitate swift packet routing at high bit rates through simple processing. The exploration of various methods for optical label encoding and decoding has been undertaken. The phase of coherent light, a characteristic of light, has proven effective in numerous optical systems, leveraging the interference behavior between multiple signals. This feature has been harnessed for label recognition techniques in photonic routers based on optical code correlation. However, many proposed systems face limitations in recognizing all binary codes since only those providing sufficient discrimination between auto-correlation and cross-correlation can be identified. Moreover, in most systems, each optical integrated circuit can recognize only a single label. Consequently, multiple correlators must be prepared at each node to recognize all routing labels.

In contrast, for the processing of multiple labels, the recognition systems utilizing a self-routing architecture for phase-shift-keying (PSK) labels have been proposed. In the literature, a demonstration of optical multiple label recognition for on-off keying (OOK) codes at 250Gbit/s using a self-routing scheme was presented [9]. The self-routing of label data streams for label recognition stands out as a promising method in label decoding systems. An additional contribution comes from our proposal of an all-optical passive label recognition system capable of recognizing all binary codes in binary PSK (BPSK) form [7]. This label recognition system comprises a tree-structure connection of passive waveguide components, referred to as an asymmetric X-junction coupler and time gates. The circuit incorporates asymmetric X-junction couplers, Y-junctions, and 3-dB directional couplers. This research proposes a new label recognition structure for Binary Phase Shift Keying (BPSK) coded label.

The functionality of the label recognition, implemented through optical integrated circuits, has been validated using the finite-difference beam propagation method (BPM) and EME. This method allows for a comprehensive understanding and confirmation of the label recognition operations within the proposed circuits.

2. Working principle of the optical BPSK label recognition

In a photonic label switching network, optical labels serve as routing information, as illustrated in Fig.1 [10]. The process involves attaching a label to an incoming packet at an edge router, which is then utilized to direct the packet to another edge router connected to the packet's destination. Within a node, routing switches are manipulated based on the label information, referencing a routing table. The initial step involves analyzing the label to determine the destination information. This necessitates inspecting whether the label aligns with any of the labels present at the routers. The efficiency of this label resolution process depends on the network's design and routing protocol. In a hierarchical network structure, a router at a node in a sub-network may only need to resolve labels corresponding to packets destined for that specific sub-network [11]. In such cases, it is not mandatory for the router to resolve all the labels across the entire network. The degree of label resolution required is contingent upon the intricacies of the network architecture and the routing protocols employed. This mechanism ensures that the optical signals are appropriately routed to their intended destinations based on the encoded information within the pulse train [12]. The number of output ports, denoted as M, corresponds to the total number of coded addresses, specifically $M=2^N$ for BPSK code, respectively.

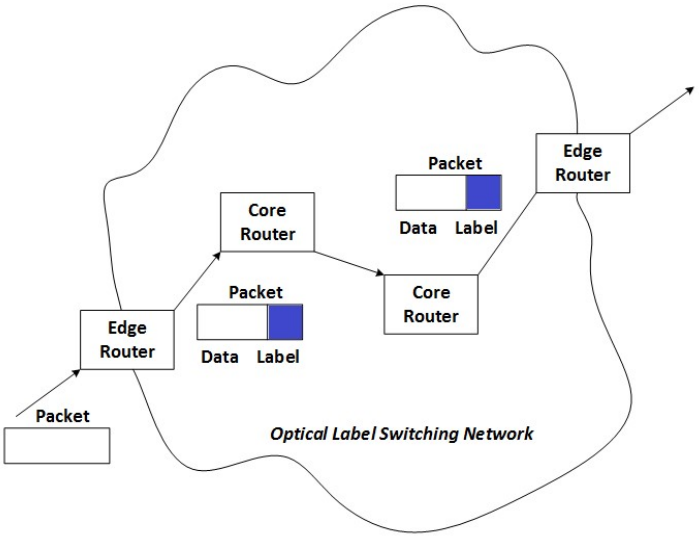

Fig 1. General structure of optical label switching networks

This relationship reflects the exponential increase in the number of potential addresses with the modulation format used. Given that all bits of the label arrive sequentially, a processing circuit is employed to parallelize all the bits at a specific time, as illustrated in Fig.2.

In this scheme, each nth-stage circuit module directs the identifying (ID) pulse to the output port aligned with the nth address pulse, utilizing the n^{th} address pulse as the control signal.

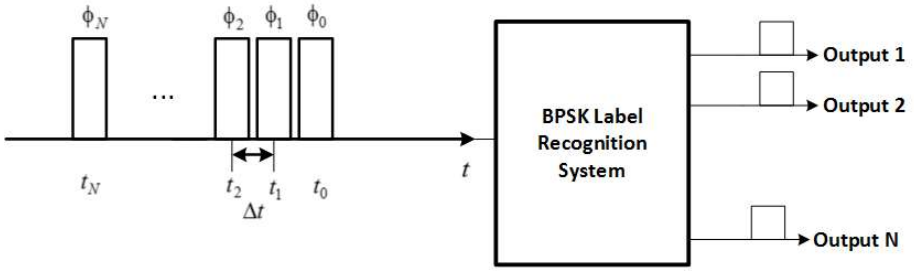

Fig 2. Principle operation of the optical BPSK label recognition system

3. Proposal of the new architecture

Several methods have been explored for representing routing label information as optical signals, encompassing coding in the time-domain, spectral domain, and combinations of these approaches [11]. In this context, we specifically examine the utilization of time sequential coded pulse trains in Binary Phase Shift Keying (BPSK) modulation format. To ensure accurate identification of their absolute phase, a reference signal is introduced, placed ahead of the pulses that signify an address. The electric field of the optical pulse train for a label with (N + 1) symbols is expressed as follows

$$E_{label}(t) = \sum_{i=0}^{N} a_i f_0(t - i\Delta t)\exp(j\phi_i)\exp(j\omega(t - i\Delta t)) \quad (1)$$

Where, the term $f_0(t)$ represents the envelope of a pulse characterized by the angular frequency ω, amplitude a_i, phase ϕ_i, and the pulse period Δt. This mathematical representation encapsulates the essential properties of the pulse in the time sequential coded pulse train.

In this research, we propose a new scheme for the optical BPSK label recognition circuit based on the SOI platform. The proposed structure is based on cascaded MMI couplers integrated as shown in Fig.1(a). In this design, we use an SOI waveguide with the following parameters: the height of 220nm and the width of 500nm. At operating wavelengths around 1550nm, the waveguide is a single mode waveguide. The cross-sectional view of the device is shown in Fig.1(b) and the profile of the optical field within the waveguide is shown in Fig.1(c).

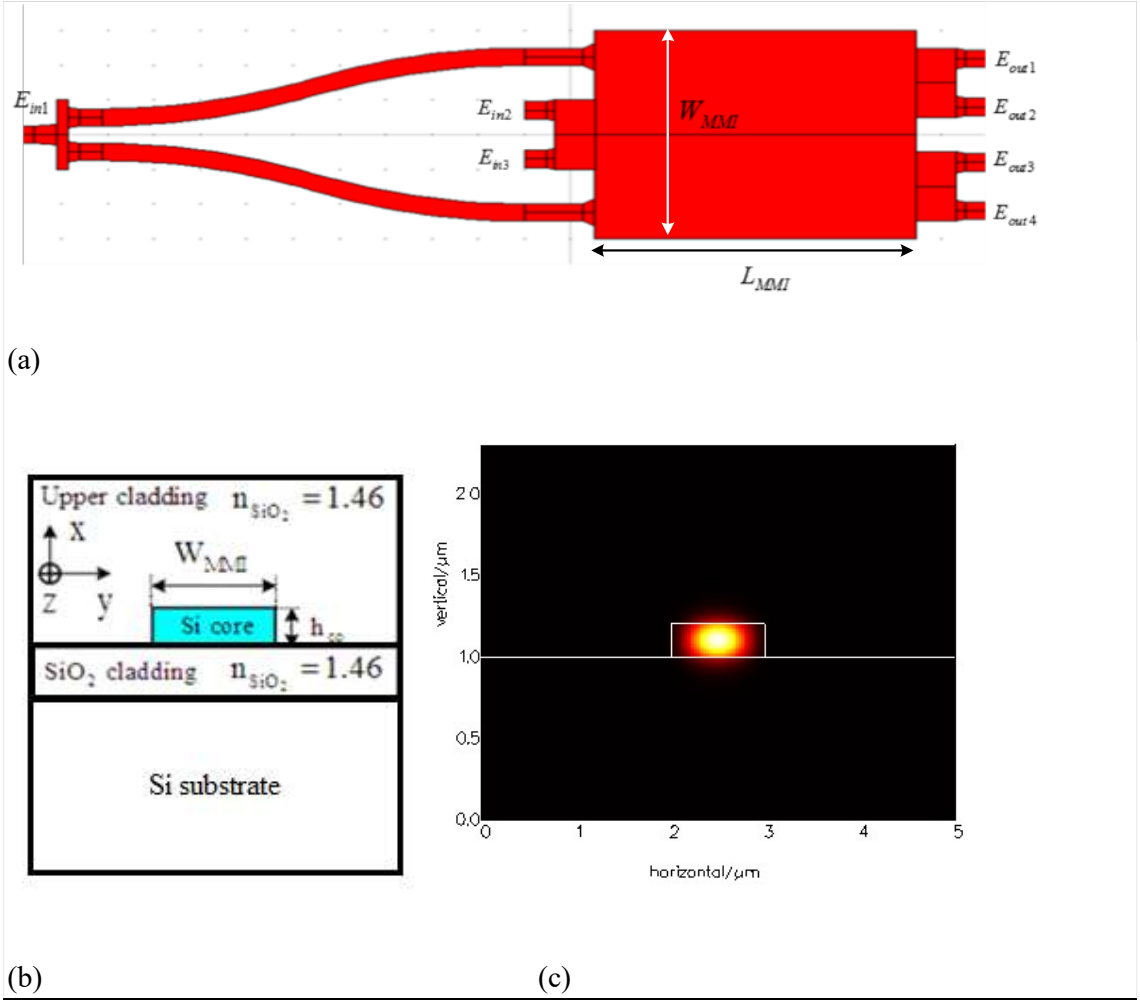

Fig 3. Optical structure based on MMIs for BPSK label recognition (a) circuit, (b) cross-sectional view and (c) field profile

The Silicon-on-Insulator (SOI) platform utilizes silicon as both the substrate and the guiding core material. The substantial index contrast between silicon (n=3.45 at a wavelength of 1550nm) and the surrounding material (n=1.46) enables effective light confinement within submicron dimensions. Single-mode waveguides within this platform can feature core cross-sections with dimensions as small as a few hundred nanometers and bend radii of a few micrometers, all while incurring minimal losses. Furthermore, the SOI technology holds the potential for the monolithic integration of electronic and photonic devices on a single substrate. This integration capability is advantageous for creating compact and efficient devices that combine both electronic and photonic functionalities within the same platform. In this study, the access waveguides are identical single mode waveguides with width W_a. The input and output waveguides are located at [13]

$$x_i = (i + 1/2)\frac{W_{MMI}}{4} \tag{2}$$

A single 4x4 MMI coupler at a length of $L_1 = \frac{3L_\pi}{4}$ is described by the following transfer matrix

$$\mathbf{M} = \frac{1}{2}\begin{bmatrix} -1 & -e^{j\frac{3\pi}{4}} & e^{j\frac{3\pi}{4}} & -1 \\ -e^{j\frac{3\pi}{4}} & -1 & -1 & e^{j\frac{3\pi}{4}} \\ e^{j\frac{3\pi}{4}} & -1 & -1 & -e^{j\frac{3\pi}{4}} \\ -1 & e^{j\frac{3\pi}{4}} & -e^{j\frac{3\pi}{4}} & -1 \end{bmatrix} \tag{3}$$

For the 2x2 MMI, the transfer matrix the transfer matrix $\mathbf{M}_{GI}$ for an ideal 2x2 general interference MMI (GI-MMI) coupler of length $3L_\pi/2$ can be expressed as

$$\mathbf{M}_{GI} = \frac{1}{\sqrt{2}}\begin{bmatrix} 1 & -j \\ -j & 1 \end{bmatrix} \tag{4}$$

By adding phase shifters at the input and output waveguides for a 2x2 GI-MMI coupler as shown in Fig.4, the overall transfer matrix for the coupler has the form required for a sum and difference unit (Haar transform) as follows

$$\mathbf{M}_{\phi} = \frac{1}{\sqrt{2}}\begin{bmatrix} 1 & 1 \\ 1 & -1 \end{bmatrix} \tag{5}$$

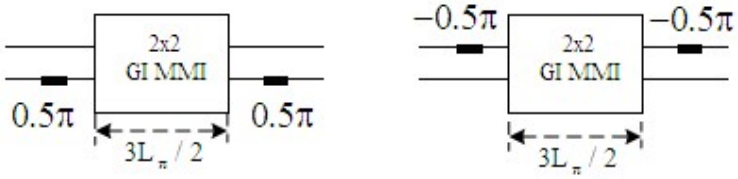

(a) *(b)*

Fig. 4 The Haar matrix based on a 2x2 GI-MMI coupler

The cascaded MMIs serve the purpose of discerning the phase of the incident wave in Binary Phase Shift Keying (BPSK) format. By implementing a cascaded connection of these MMI couplers, the system can effectively identify two-bit addresses. The relationship between the input and output fields within this cascaded arrangement is a critical aspect of the operation. The specific nature of this relationship, including equations or further details, is likely to be

described in the complete context of the original document.

$$\begin{pmatrix} E_{out1} \\ E_{out2} \\ E_{out3} \\ E_{out4} \end{pmatrix} = \begin{pmatrix} 1 & -1 & 1 \\ -1 & 1 & 1 \\ 1 & 1 & 1 \\ -1 & -1 & 1 \end{pmatrix} \begin{pmatrix} E_{in1} \\ E_{in2} \\ E_{in3} \end{pmatrix} \tag{6}$$

When an optical two-bit Binary Phase Shift Keying (BPSK) pulse train is introduced, the normalized intensity of the pulse trains is observed emanating from four output ports. This presentation suggests that the proposed circuit, designed for discerning phase information in a BPSK format, results in the distribution of optical intensity across multiple output ports. The specifics of the intensity distribution and any numerical values or additional details would likely be provided in the complete context of the original document.

3. Simulation Results

The 2-point Haar transform unit can be realized through the utilization of a 2x2 Grating-Image Multimode Interference (GI MMI) coupler, assisted by phase shifters, with a primary focus on optimizing these components on the Silicon-on-Insulator (SOI) platform. The waveguide structure, as depicted in Fig. 1(b), incorporates Silicon as the upper cladding, with a waveguide width of 500nm and a thickness of 220nm. The initial phase of optimization involves fine-tuning the Multimode Interference (MMI) sections. Tapered waveguides, with a specified length, are employed to connect the access waveguides to the MMI sections, aiming to enhance overall device performance. Ensuring that the multimode sections are sufficiently wide is crucial for achieving optimal performance, and proper spacing is maintained to minimize crosstalk between adjacent access waveguides. The optimization process begins with 3D-BPM simulations for the 2x2 GI-MMI coupler, utilizing a specific length (length not explicitly mentioned). The objective at this stage is to identify approximate positions that result in a power splitting of 50/50, equivalent to a 3dB coupler. Subsequently, more detailed 3D-BPM simulations are conducted around these initially identified positions. This refinement step is undertaken to pinpoint the best lengths for the various components, ensuring optimal performance of the 2x2 GI MMI coupler.

To attain a device that is both compact and high-performing, efforts are directed towards minimizing the separation between parallel access waveguides while ensuring it remains sufficiently large to control power coupling between adjacent input and output waveguides. Employing two parallel tapered waveguides as a directional coupler, the adiabatic design of the tapers ensures that only the fundamental local normal mode carries power, estimating power coupling between the fundamental modes of the tapered waveguides. Through BPM simulations, the width of the Multimode Interference (MMI) is optimized at 6 μm for a compact and high-performance device. Exploring the impact of MMI length on device performance, assessments are made for excess loss and imbalance in a 4x4 MMI coupler. Fig.

5(a) presents 3D-BPM simulation results, including normalized output powers, excess loss, and imbalance. The optimized length of each MMI coupler is determined. At this specific length, excess loss and imbalance are calculated to be 0.58 dB and 0.01 dB, respectively. Simulation results in Fig. 5(b) showcase field propagation within the MMI coupler at the optimal length for signals at input ports 1 and 2. Notably, simulations reveal a substantial fabrication tolerance for the MMI coupler. Specifically, the fabrication tolerance for the MMI length is ±100 nm for a normalized output power variation of 0.01, a margin easily achievable through methods such as e-beam or 193 nm deep UV lithography.

Subsequently, an examination is conducted to assess the width tolerance and wavelength sensitivity, or bandwidth, of the device. Simulations reveal that a deviation from the operating wavelength of 1550nm results in a decrease in the normalized output power of the MMI coupler. This decline is attributed to the inverse proportionality of the beat length of the MMI coupler to the wavelength. The bandwidth, defined at 85% total transmittance (-1dB from the maximum), is found to be approximately inversely proportional to the MMI length. Within the -1dB bandwidth, the variation in normalized output powers is determined to be less than 0.01. 3D BPM simulation results indicate that the -1dB bandwidth of the MMI coupler spans 35nm over a wavelength range from 1532nm to 1567nm. Within a 15nm wavelength span around the operating wavelength of 1550nm, the simulations illustrate that the normalized output powers at output ports 1 and 4 of the MMI coupler closely align with the 50:50 target [14]. This analysis provides insights into the device's performance under varying wavelengths and underscores its ability to maintain the desired output characteristics within a specific wavelength range.

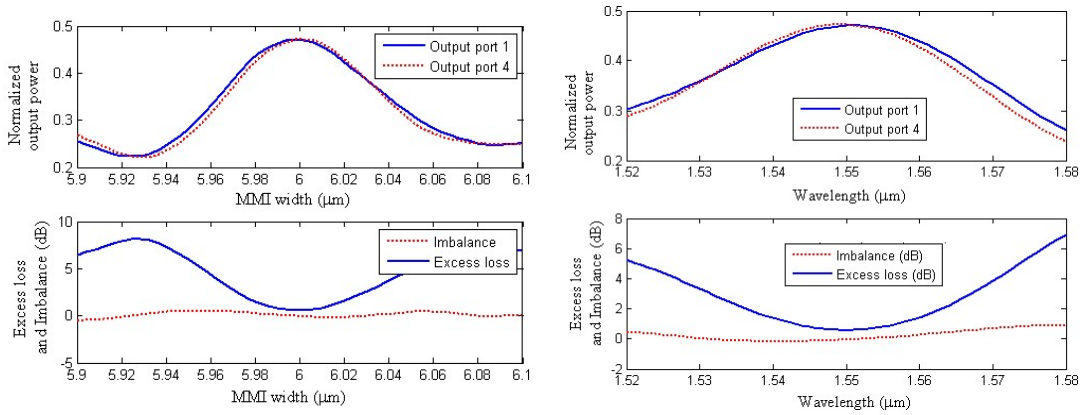

(a) (b)

Fig. 6. BPM simulation results of the normalized output powers, excess loss and imbalance of the 4x4 MMI coupler as the function of (a) MMI width and (b) optical wavelength

The normalized output powers at different lengths of the 1x2 MMI are shown in Fig.7. The optimal length of the coupler is 4.9 μm.

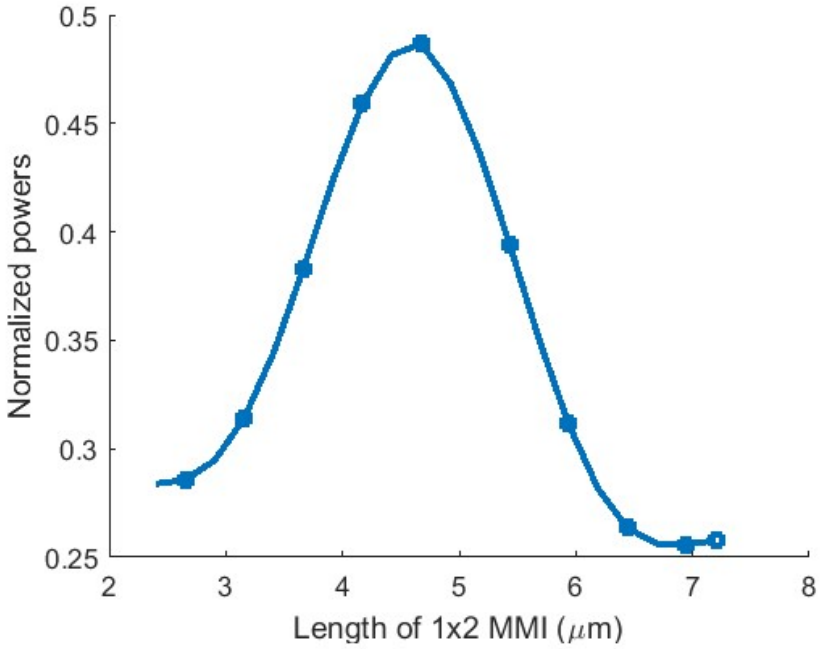

Fig. 7. BPM simulation results of the normalized output powers of 1x2 MMI

In this research, the phase shifters can be designed by using 1x1 MMI couplers. Using the MPA method, the field at distance z along the multimode section can be written as [15]

$$\Psi(y, z=L) = e^{-j\beta_{0M}z}\sum_{\upsilon=0}^{M-1} c_\upsilon \phi_y(y)\exp[j\frac{\upsilon(\upsilon+2)}{3L_\pi}] = e^{-j\beta_{0M}z}\Psi(y, z=0) \quad (7)$$

Therefore, the difference of the relative phase between two arms of the MZI is $\Delta\varphi = (\beta_{0M} - \beta_0)L_M$, where β_0 and β_{0M} are the propagation constants of the fundamental modes of the single and multimode sections.

The BPM simulations show that when an optical two-bit BPSK pulse train is introduced, the normalized intensity of the pulse trains is observed emanating from four output ports as shown in Fig. 8.

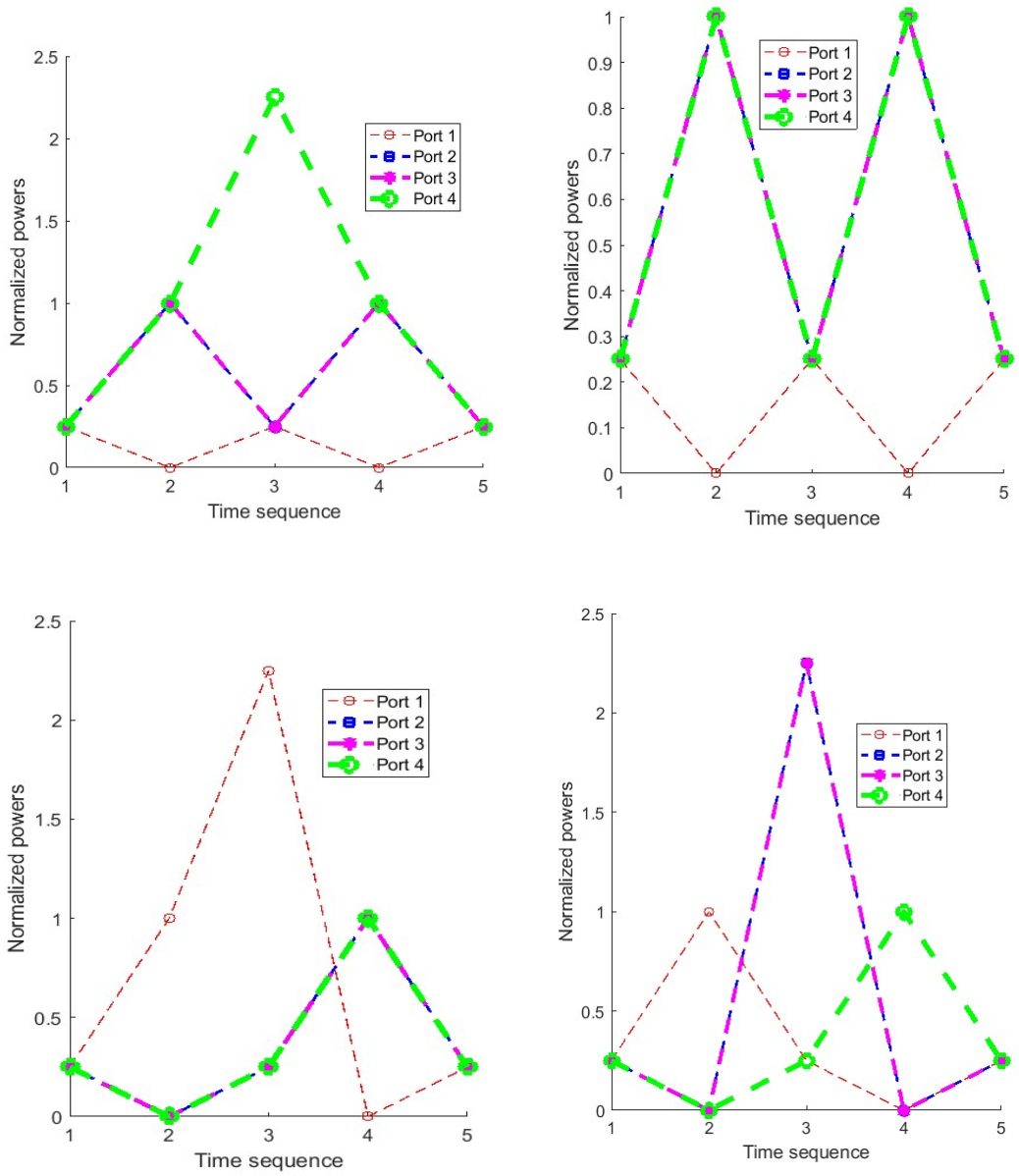

Fig. 8 BPM simulations for normalized powers at output ports 1, 2, 3 and 4 for address (b) 00, (c) 0-pi, (d) pi-0 and (e) pi- pi

By using the BPM simulation, the fields propagated via the whole device for addresses 00, 0π, $\pi 0$, $\pi\pi$ are presented in Fig.9. The simulation results show that the analysis has a good agreement with the numerical simulations.

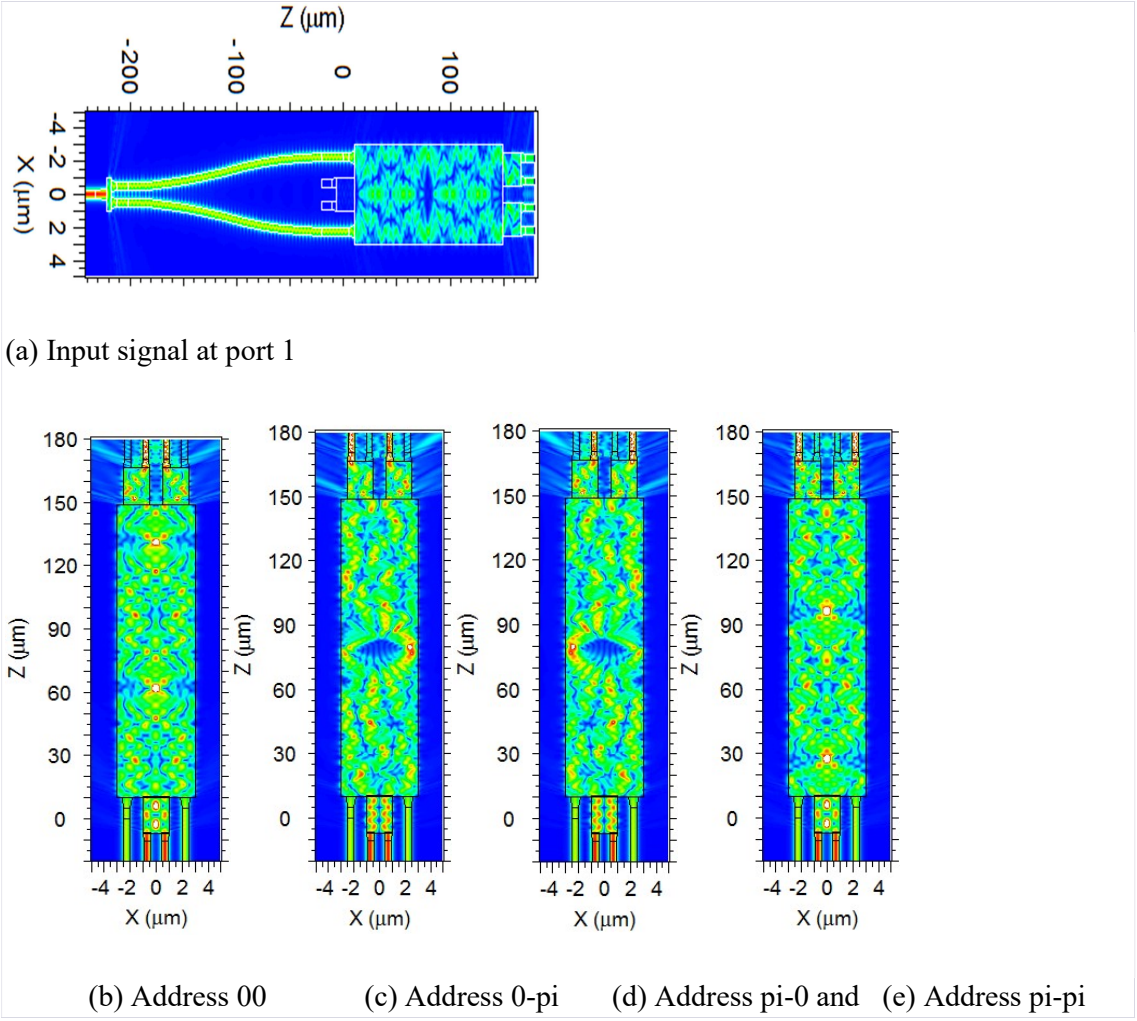

(a) Input signal at port 1

(b) Address 00 (c) Address 0-pi (d) Address pi-0 and (e) Address pi-pi

Fig. 8 BPM simulations for (a) input signal at port 1 and for cases of address (b) 00, (c) 0-pi, (d) pi-0 and (e) pi- pi

4. Conclusions

We have presented a new optical circuit based on multimode interference (MMI) structures for the recognition of Binary Phase Shift Keying (BPSK) coded label. Our circuits employ 1x2, 4x4 and 2x2 cascaded MMIs. The design is based on the silicon on insulator (SOI) platform, which is suitable for the existing CMOS technology. As a result, our new proposed design has advantages of low loss, compactness, high bandwidth and large fabrication tolerance compared to the recent research published in the literature based on X-junction couplers. The fabrication tolerance for the MMI length is ±100 nm and the bandwidth is about 15nm. The proposed sensor structure can be integrated with all optical label switching networks.

Acknowledgement

This research is funded by the Ministry of Science and Technology of Vietnam under pro-ject number ĐTĐL.CN-92/21.

References

[1] Y. Ohkubo, H. Kishikawa, and J. Fujikata, "Optical Label Recognition for Two-Symbol QPSK-Coded Labels Using Complex-Valued Neural Network," in *2023 28th Microoptics Conference (MOC)*, 24-27 Sept. 2023 2023, pp. 1-2, doi: 10.23919/MOC58607.2023.10302878.

[2] T. Yang *et al.*, "Optical Labels Enabled Optical Performance Monitoring in WDM Systems," *Photonics*, vol. 9, no. 9*,* doi: 10.3390/photonics9090647.

[3] V. Agarwal, P. Pareek, L. Singh, B. Balaji, P. K. Dakua, and V. Chaurasia, "Design and analysis of all optical header recognition system employing combination of carrier reservoir SOA and conventional SOA," *Optical and Quantum Electronics,* vol. 56, no. 1, p. 83, 2023/12/02 2023, doi: 10.1007/s11082-023-05657-0.

[4] K. S. Chen, "Implicit Label Number for Optical Packets in Label Switching Networks Based on Spectral Amplitude Coding and OCDM Path," *IEEE Photonics Journal,* vol. 14, no. 4, pp. 1-7, 2022, doi: 10.1109/JPHOT.2022.3188164.

[5] A. Ihara, H. Kishikawa, N. Goto, and S. I. Yanagiya, "Passive Waveguide Device Consisting of Cascaded Asymmetric X-Junction Couplers for High-Contrast Recognition of Optical BPSK Labels," *Journal of Lightwave Technology,* vol. 29, no. 9, pp. 1306-1313, 2011, doi: 10.1109/JLT.2011.2124442.

[6] Q. Zhang, X. Gong, and L. Guo, "All-Optical QPSK Pattern Recognition in High-Speed Optoelectronic Firewalls," *IEEE Photonics Journal,* vol. 15, no. 2, pp. 1-16, 2023, doi: 10.1109/JPHOT.2023.3243896.

[7] H. Kishikawa, A. Ihara, N. Goto, and S.-i. Yanagiya, "Increase of Recognizable Label Number with Optical Passive Waveguide Circuits for Recognition of Encoded 4- and 8-Bit BPSK Labels," *IEICE Transactions on Electronics,* vol. E100.C, no. 1, pp. 84-93, 2017, doi: 10.1587/transele.E100.C.84.

[8] T. Segawa, S. Ibrahim, T. Nakahara, Y. Muranaka, and R. Takahashi, "Low-Power Optical Packet Switching for 100-Gb/s Burst Optical Packets With a Label Processor and 8 × 8 Optical Switch," *Journal of Lightwave Technology,* vol. 34, no. 8, pp. 1844-1850, 2016, doi: 10.1109/JLT.2015.2512844.

[9] I. Kensuke, H. Yoshimitsu, K. Hiroki, and G. Nobuo, "Noise tolerance in optical waveguide circuits for recognition of optical 16 quadrature amplitude modulation codes," *Optical Engineering,* vol. 55, no. 12, p. 126105, 12/1 2016, doi: 10.1117/1.OE.55.12.126105.

[10] V. Andrushchak, M. Beshley, L. Dutko, T. Maksymyuk, and T. Andrukhiv, "Intelligent Traffic Engineering for Future Intent-Based Software-Defined Transport Network," in *Future Intent-Based Networking*, Cham, M. Klymash, M. Beshley, and A. Luntovskyy, Eds., 2022// 2022: Springer International Publishing, pp. 161-181.

[11] Y. Yan, "A Research on Key Technologies in All-Optical Label Switching Networks," *Journal of Physics: Conference Series,* vol. 1710, no. 1, p. 012007, 2020/11/01 2020, doi: 10.1088/1742-6596/1710/1/012007.

[12] T. Kodama and G. Cincotti, "Hybrid QAM-Based Labels Generated by Two Multi-Level PSK Codes," *IEICE Transactions on Communications,* vol. E102.B, no. 12, pp. 2199-2204, 2019, doi: 10.1587/transcom.2019EBP3024.

[13] J. M. Heaton and R. M. Jenkins, " General matrix theory of self-imaging in multimode interference(MMI) couplers," *IEEE Photonics Technology Letters,* vol. 11, no. 2, pp. 212-214, Feb 1999 1999.
[14] T.-T. Le and L. Cahill, "Generation of two Fano resonances using 4x4 multimode interference structures on silicon waveguides," *Optics Communications,* vol. 301-302, pp. 100-105, 2013.
[15] T.-T. Le, *Multimode Interference Structures for Photonic Signal Processing*. LAP Lambert Academic Publishing, 2010.